https://doi.org/10.1016/j.measurement.2018.10.012

Influence of laser tracker noise on the uncertainty of machine tool volumetric verification using the Monte Carlo method

P. Pérez[(1)*], S. Aguado[(2)], J.A. Albajez[(1)], and J. Santolaria[(1)]

[(1)] Department of Design and Manufacturing Engineering, University of Zaragoza, 50018 Zaragoza, Spain. pperezm@unizar.es

[(2)] Centro Universitario de la Defensa. Universidad de Zaragoza. Academia General Militar, Ctra. Huesca s/n 50090 Zaragoza, Spain.

ABSTRACT

Verification of workpieces is typically performed in the post-process with coordinate measuring machines, thereby increasing the manufacturing cycle time. However, machine tools presently can perform contact measuring operations by using a probe. Moreover, there is a growing need for in-process inspection of workpieces. Therefore, using the machine tool itself for the verification whilst the workpiece remains clamped to the machine can lead to an improvement in manufacturing efficiency, cost reduction, higher energy saving and better equipment productivity. However, the use of touch probes as a measurement tool in manufacturing requires some preparatory works. Firstly, the accuracy of the machine tool should be improved to reduce the influence of its geometric errors. Secondly, the uncertainties in calibration and measuring procedure should be determined to obtain the measurement uncertainty. This study presents a new tool that can analyse the effect of different verification parameters in calibration uncertainty based on Monte Carlo method. On the basis of the actual tests performed on a milling machine and its geometric errors, the effect of laser tracker measurement noise in calibration uncertainty is investigated.

Keywords: Machine Tool; Measurement; Uncertainty; Monte Carlo; Volumetric Verification; Laser Tracker noise.

1. Introduction

Industrial sectors such as aeronautics, automotive, renewable energy and nuclear power, demand manufacturing of components with high accuracy but with minimum costs. The transportation of these components to an environmentally controlled metrological laboratory leads to an increase in manufacturing time, thereby increasing the manufacturing costs. The integration of the workpiece verification process into the machine tool (MT) can reduce the manufacturing time because transportation is not necessary. Moreover, whilst the workpiece remains clamped to the MT, the same coordinate system utilised during the manufacturing process can be used for the measurements and rework. Hence, manufacturing time and machining waste materials are significantly reduced, thereby minimising the costs without affecting the product quality. To reach this goal, traceable dimensional metrology techniques must be incorporated in the MT to ensure that the resultant manufacturing program can produce the required output within the specified tolerance [1].

Through MT calibration, the influence of MT's combined geometric errors is determined. Thus, the MT accuracy is increased and the influence of these systematic errors is reduced through software compensation. The MT geometric error is the difference between the actual response of the MT to a command issued according to the accepted protocol of that machine's operation and the response anticipated by that protocol [2]. Errors are broadly classified into the following two categories: quasi-static and dynamic [3]. Quasi-static errors are those between the tool and workpiece and are related to the structure of the MT. These errors gradually vary with time, caused by sources such as geometric, kinematic and thermally induced errors. Meanwhile, dynamic errors are caused by sources such as spindle error motion, vibrations and controller errors [4]. Each axis of an MT movement can be described by six degrees of freedom, that is, three translations and three rotations. Thus, a three-axis MT has 21 components of geometric and kinematic errors, that is, six errors per axis plus a squareness

https://doi.org/10.1016/j.measurement.2018.10.012

error between each pair of axes. The notation of the geometric errors is standardised in accordance with the International Organization for Standardization (ISO) 841 [5] and VDI 2617-3 [6].

Each geometric error can be measured individually via direct measurement techniques, or the combined errors can be determined using indirect measurements. UNE-ISO 230-1:2014 [7] is an international standard that specifies the methods for testing the accuracy of MTs by using direct measurements, operating under either no-load or quasi-static conditions. By using direct measurement, the influence of each error of each axis is determined in a particular position in the workspace of the MT [3]. By using indirect measurement methods, the combined influence of MT geometric errors is determined on the basis of the multi-axis movement and MT kinematic model [8,9]. Trapet *et al.* [10] proposed in 1991 a method for evaluating all error parameters for three-axis machines by using only a 2D reference object. Whilst direct measurement provides the actual physical behaviour of each error, indirect measurement provides an interrelated set of optimal values. However, with indirect measurements, the relationship between the geometric errors is not investigated, and the approximation functions obtained are directly extrapolated to the entire MT workspace. Similarly, each error needs its own assembly measurement procedure and data processing, hence substantially increasing the verification time. These are the main reasons why volumetric verification based on indirect measurements that use laser tracer [11-13], laser tracker (LT) [14-16], or ball bar [17] as measurement systems is more popular than geometric verification based on direct measurements that use laser interferometer, levels, etc., particularly for evaluating long-range MTs.

MT verification process improves the measurement capability, as well as the associated verification uncertainty value. It characterises the dispersion of results in relation to the geometric errors obtained and the sources of errors that affect them. This verification process is considered particularly in different manufacturing and quality assurance processes [18, 19]. This process is also required when the MT is used as the first step in the measurement system to obtain a traceable measurement system.

The ISO has developed and published various guidelines for the representation of measurement uncertainty, such as the UNE-ISO/TR 230-9 [20] standard for measurement uncertainty estimation for machine tool test and ISO/TS 14253-2 [21], which are widely accepted. These standards combine the estimation of different error sources and their associated typical uncertainties to determine the uncertainty associated with the overall process. Thus, the accuracy and metrological characteristics of an MT as a measurement system are related to the measurement system, MT and calibration conditions used. The “Guide to the expression of uncertainty in measurement” (GUM) [22] provides the basic framework for evaluating the uncertainty in measurement, but it is not suitable in nonlinear processes such as MT calibrations based on volumetric verification. The Monte Carlo method is recommended to obtain the uncertainty for each point of the MT workspace in the case of a 3D measurement system. The obtained shape is ellipsoid with axes $u_x(P)$, $u_y(P)$ and $u_z(P)$. The ellipsoid represents the volume in which determining the true value of the measured point is possible.

In metrology, the value of a measurement must be given with its uncertainty value. The uncertainty value is a quantitative indication of the quality of the measurement result. Recent research has focused on the study of uncertainty of MTs and coordinate measuring machines (CMMs). Liebrich *et al.* [23] used a simulation to investigate the influence of geometric errors of the CMM on the calibration of a 3D ball plate. Jankowski and Woźniak [24] proposed the use of master artefacts in 2D and 3D for testing the performance of probes for MTs and CMMs. Radlovački *et al.* [25] used the Monte Carlo method to evaluate the uncertainty in measuring flatness based on the repeatability of sample coordinates of a point.

This study uses a simulation software developed by the authors to verify how the different factors with influence on the volumetric verification affect the calibration uncertainty. The software allows the use of different probabilistic distribution functions (PDFs) to characterise the behaviour of each error source. Among the various uncertainty sources, this study focuses on the influence of LT measurement noise. Hence, actual tests are performed using a milling machine with the XFYZ configuration, an LT (Leica LTD 600) as the external measurement system, a touch probe as the onboard measurement system and the software developed by the authors.

https://doi.org/10.1016/j.measurement.2018.10.012

2. Comparison of GUM and Monte Carlo methods to determine the uncertainty of MT volumetric verification process

2.1 Volumetric verification and influencing factors

Volumetric verification is based on an intensive process of identification of parameters by using a kinematic model of the MT. By minimising the difference between the theoretical and actual pairs of points by using the MT kinematic model, the combined influence of MT geometric errors is obtained. Their behaviours are modelled, and the mean square volumetric error of the machine (Ve_{LT}) is minimised using nonlinear optimisation techniques [8].

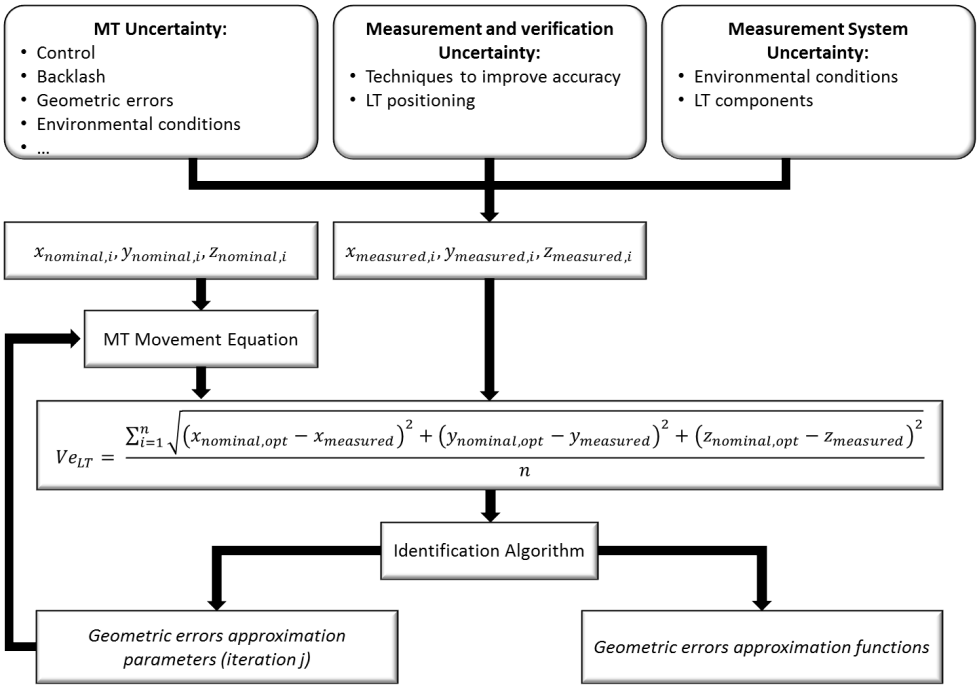

Figure 1. *Volumetric verification scheme considering uncertainty sources*

As shown in Figure 1, the principal uncertainty sources that influence MT verification are divided into three groups, namely, MT, measurement and verification and measurement system uncertainties.

2.2 Main differences between GUM and Monte Carlo methods

The GUM provides a framework for evaluating and expressing measurement uncertainty. Supplement 1 to the GUM describes the problem of uncertainty evaluation in terms of probability density functions. It provides the procedure to obtain the best estimate.

Whilst the GUM focuses on evaluating Type A, Type B and combined uncertainties, the Monte Carlo method uses a large number of samples, with different probabilistic functions, to obtain the final uncertainty distribution through the measurement equation (Figure 2). The Monte Carlo method uses the computational capacity of modern computers to simulate a large number of pseudo random numbers. Thus, it allows simulation of complex systems from a probabilistic point of view [26].

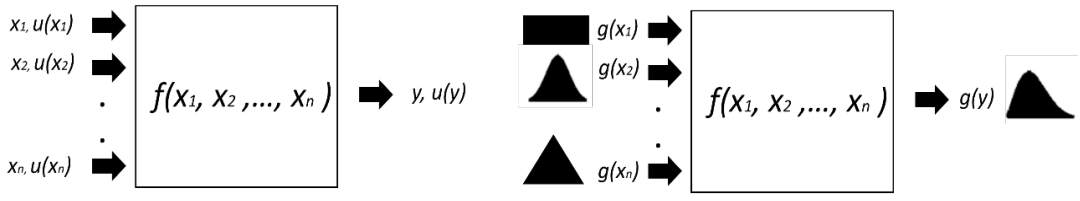

https://doi.org/10.1016/j.measurement.2018.10.012

Figure 2. *Left: Propagation of uncertainties based on the GUM. Right: Propagation of distribution based on the Monte Carlo method.*

However, the estimation of uncertainties by using the GUM relies on assumptions that are not always fulfilled. The adequacy limitations of the GUM are as follows:

- The mathematical model that describes the process is nonlinear. When the model presents strong elements of nonlinearity, the approximation made by the GUM approach may not be sufficient to estimate the uncertainty value correctly.
- The central limit theorem states that, in most situations, the combination of a large number of distributions results in a normal distribution. However, the resultant distribution in various actual cases presents an asymmetric behaviour, thus invalidating the assumption used in the central limit theorem.
- The expanded uncertainty calculated by the GUM does not always present an analytical solution.
- The input quantities are not symmetrical, or some of the input sources are much larger than the others.
- The order of magnitude of the estimated output variable and that of the associated standard uncertainty are approximately the same.

Supplement 1 of the GUM provides the steps to be followed when the Monte Carlo method is used (Figure 3).

Figure 3. *Sequence of steps when Monte Carlo method is used*

1. Definition of the measurand and input quantities: Several sources of uncertainty affect the MT volumetric verification. The principal contributions are uncertainty associated with the MT (e.g. environmental conditions, MT characteristics, etc.), uncertainty related to the measurement system (e.g. measurement and components uncertainty, influence of environmental conditions, etc.) and uncertainty associated with the measurement technique and optimisation strategy (e.g. identification algorithm, sequence, etc.).
2. Modelling: Volumetric verification identifies the influence of MT geometric errors through its movement equation, that is, the kinematic model of the MT. Therefore, the physical components, such as joints and guides, that generate the movement of the MT should be modelled.
3. Estimation of PDFs for the input quantities: Once input quantities are defined (first step), based on state-of-the-art (the highest level of development) and empirical results, the PDF that estimate the input quantities should be defined.
4. Setting up and running the Monte Carlo simulation: After completing the previous steps, the MT verification process is simulated using the software developed by the authors. The total number of simulations to be implemented is defined by the user, as well as the uncertainty related to the measurement technique and optimisation strategy.
5. Summary and results: When all the MT simulation verification tests have been completed, the first parameter to be analysed is the probability distribution of the initial volumetric error. Later, the analysis is performed with the final volumetric error. Moreover, the uncertainty of each point and adequacy of the approximation functions obtained can also be observed and analysed.

https://doi.org/10.1016/j.measurement.2018.10.012

3. Methodology

The ISO/TS 15530-3:2011 standard [27] provides an experimental technique for the uncertainty evaluation of task-specific CMM measurements by using calibrated workpieces. It describes the uncertainty evaluation procedure for both parts, namely, experiment and calculation. Given that the main idea is to use the MT as a CMM, using this standard is appropriate. The equation used for the calculation of the expanded uncertainty is

$$U = k \cdot \sqrt{u_{cal}^2 + u_p^2 + u_b^2 + u_w^2}, \tag{1}$$

where u_{cal} is the standard uncertainty associated with the calibrated workpiece, u_p is the standard uncertainty resulting from the measurement procedure of that calibrated artefact in the MT, u_b is the standard uncertainty associated with systematic errors, u_w is the standard uncertainty resulting from material and manufacturing variations (owing to the variations in the expansion coefficient, form errors, roughness and elasticity) and k is the coverage factor (typically for $k = 2$, the level of confidence is 95%).

The first term, u_{cal}, should be stated in the calibration certificate. Alternatively, it can be estimated from the maximum permissible error (MPE) of the CMM used for the calibration of the workpiece ($u_{cal,MMC}$) [21]. The uncertainty caused by thermal drifts (u_T), derived from the expansion of the reference artefact, is negligible in the present study because the calibration was performed under controlled environmental conditions.

$$u_{cal} = \sqrt{u_{cal,MMC}^2 + u_T^2}, \tag{2}$$

where

$$u_{cal,MMC} = 1.45 + \frac{L}{500}. \tag{3}$$

Here, L is expressed in millimetres and the final value is in micrometres.

The value of u_p, the uncertainty related to the measurement procedure, can be calculated for each position of the workspace two times the standard deviation of the simulated mesh of points at that position. In the present case, this value will be calculated in Section 4 (“Experimental procedure and results”).

According to the GUM [22], u_b is calculated as type A uncertainty as expressed as follows:

$$u_b = \frac{\sigma}{\sqrt{n}}, \tag{4}$$

where σ is the standard deviation of the systematic error b and n is the number of simulated values. The value of u_b can be neglected because the value of σ is small and $n = 1000$ (number of the simulated Monte Carlo data).

The value of u_w has to be estimated. To reduce this term, the thermal expansion must be compensated. Then, the uncertainty u_w will be related to the accuracy of the sensor used for measuring the temperature of the plate with holes.

$$u_w = \frac{\Delta L}{\sqrt{3}} = \frac{\alpha \cdot \Delta T \cdot L}{\sqrt{3}} \tag{5}$$

If the MT user does not measure the temperature of the workpiece and compensate the effect of thermal expansion, then this lack of information should be added in this term for uncertainty.

4. Experimental procedure and results

The above methods and procedures are applied on a three-axis MT with the XFYZ configuration. The MT is an ANAYAK VH-1800 with computer numerical control (CNC) Fagor 8025, and a workspace with dimensions of 0 mm ≤ X ≤ 1500 mm, 0 mm ≤ Y ≤ 600 mm and 0 mm ≤ Z ≤ 500 mm. However, the

methods presented in this study can be used in different MT configurations regardless of the number and sequence of the MT axes.

First, when the measurement capability of an MT is to be obtained, the following questions should be answered: whether the MT is verified and its geometric errors are compensated or not, how the MT compensates its geometric errors, and which control system is used in the MT. Therefore, the measurement uncertainty will be different depending on the starting point used.

In the present case, the MT software has integrated an error compensation table that can only compensate the position errors to improve the accuracy. However, during the tests conducted in this study, the compensation matrix was disabled to identify the MT geometric errors accurately.

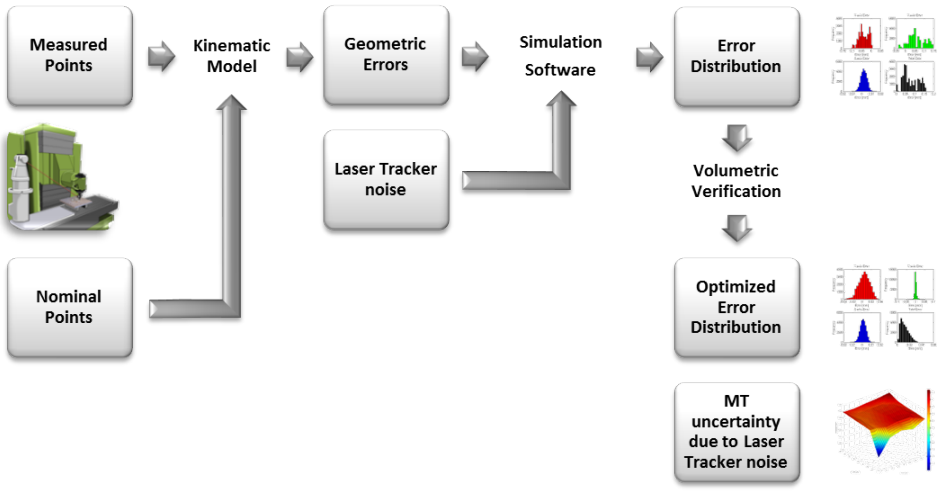

Figure 4. *Procedure to calculate the uncertainty*

Indirect measurements based on LT use automatic detection to determine the points to be captured in the workspace of the MT. The discretisation of the workspace is realised using a set of points, namely, trajectories, meshes, or a cloud of random points. Therefore, the MT workspace, to be identified as the measurement volume, is defined according to user specifications.

Because of the characteristics of the parts frequently manufactured in this machine, the MT workspace used as a measurement area is defined approximately in the middle of the XY plane, with a translational vector between the MT and part origin and dimensions of -621.133 mm in the X-axis, 606.38 mm in the Y-axis and 387.249 mm in the Z-axis. The object to be measured as the workpiece is a calibrated plate with holes (Figure 5). It is made from aluminium and has external dimensions of 460 x 460 mm. The nominal distance between the centres of the rings is 50 mm. Hence, identifying the coefficient of the thermal expansion of the plate ($\alpha_{plate} = 24 \cdot 10^{-6}\ K^{-1}$) and monitoring the plate temperature during the measurements are important to compensate possible errors owing to thermal expansion.

https://doi.org/10.1016/j.measurement.2018.10.012

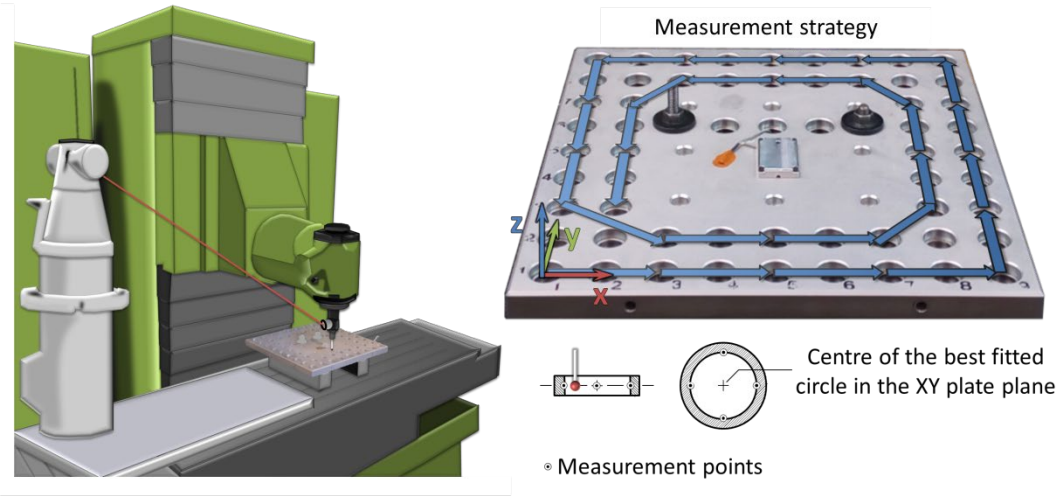

Figure 5. *Measurement configuration and strategy*

Thermal influence may be one of the most relevant uncertainty sources in a shop floor. However, in the present case, the plate was clamped on to the MT the day before performing the measurement to ensure that it is thermally stabilised and the influence of thermal gradients between the MT structure and the plate is reduced. In the same way, the LT was switched on well before performing the measurements, because the LT has been verified to have a thermal stabilisation period of at least four and a half hours [28]. Thus, the effects of thermal gradients in the structure of the LT and consequently the influence on the measured points are avoided. Similarly, ASME B5.54-2005 [2] recommends that the machine should be switched on to reach the *cold state of the machine*. That is, the machine in this state is in a stable operating temperature in which in the last 2 h period, the hydraulic systems and servos have been switched on, the spindle has not been rotated at speeds more than 10% of the maximum permissible rotations per minute and the axes' motions have been restricted to only those necessary to set up the measurement equipment. In the present case, this time was 2 hours before starting the measurements.

The calibrated plate consists of 56 holes, although only 28 holes need be measured. Thus, enough information is available to obtain the MT volumetric error and simulate the measurement of different lengths in the XY measurement area. The centres of the holes are the calibration points; therefore, four points are measured for each hole to determine the best-fitted circle centre. Each point is measured at the same time by the MT using a touch probe and by the LT using a retro-reflector magnetically attached to the probe. When the probe makes contact with the plate at the point to be measured, the MT pauses to ensure that the LT can also measure the same point, but with an offset. Because this MT has been previously investigated with regard to depth, the influence of this offset between the probe and the retro-reflector on rotational errors can be neglected. Meanwhile, the offset in the Z-axis is absorbed in the translation matrix that relates the LT and the part coordinate system (Eq. 9).

The origin of the part coordinate system is set at the centre of the first hole. The holes are measured in a spiral path, as shown in Figure 5, because it has been proven that the backlash effect on the centre of the coordinates is reduced using this method.

With measurements of four points, the centre of the best-fitted circle is calculated for each hole. Because the plate is misaligned with respect to the axis of the MT, rotating the coordinates through a rotation matrix is necessary.

$$R = \begin{bmatrix} cos\theta & sin\theta & 0 \\ -sin\theta & cos\theta & 0 \\ 0 & 0 & 1 \end{bmatrix}, \tag{6}$$

where θ is the angle of misalignment between the measured and nominal coordinates. However, to compare the measurements with their nominal coordinates, which are referenced to the plate at 20 °C (293.15 K), compensating for the thermal expansion of the plate is necessary. For simplicity, a linear behaviour is considered, starting from the clamping point (which is located at the position X = 200 mm, Y = 250 mm). The corrected distance is calculated using the following equation.

https://doi.org/10.1016/j.measurement.2018.10.012

$$d_f = d_0 \cdot \left[1 + \alpha_{plate} \cdot \left(T_{plate} - 293.15\right)\right], \tag{7}$$

where d_0 and d_f are the distances between the clamping point and centre of the hole before and after applying the correction, respectively; α_{plate} is the coefficient of the plate thermal expansion; and T_{plate} is the temperature of the plate in Kelvin during the measurement of the hole.

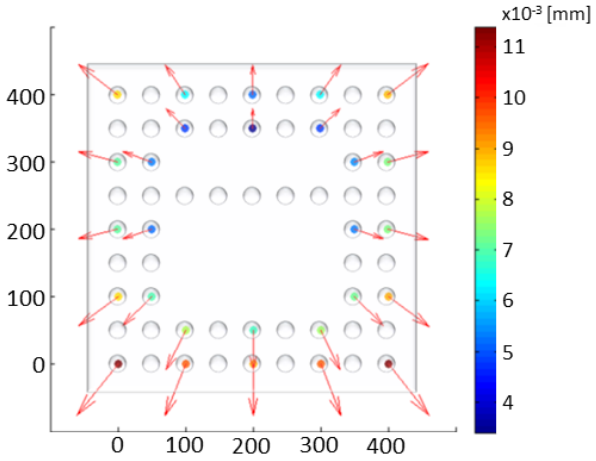

Figure 6. *Correction of the thermal expansion*

Because the misalignment and thermal expansion of the plate are not MT errors, they should be compensated to render the possibility of the comparison between the nominal and coordinates measured with the MT. Given that the measurements are performed under quasi-static conditions, the error obtained will be the result of the MT geometric, kinematic and thermally induced errors.

As shown in Figure 4, the nominal points are obtained from the calibrated plate coordinates, and the measured points are used to calculate the centres of the holes (measurement values are obtained from the LT and touch-trigger probe system). However, to determine the actual influence of MT geometric errors, an equation of motion that links the geometric errors and movement of the MT is required. Thus, defining and obtaining the kinematic model of the MT are necessary for which the volumetric verification is to be conducted (Figure 1).

As previously mentioned, the MT has the XFYZ configuration. The equation for the movement that relates the nominal coordinates of the MT with the measured coordinates of the LT through MT geometric errors and MT characteristics is presented in Eq. 8.

$$\overline{X_{LT}} = \overline{R_{LT}^{-1}}\left(\overline{R_X^{-1}}\left(\overline{R_y}\left(\overline{R_z}\,\overline{T} + \bar{Z}\right) + \bar{Y} - \bar{Z}\right) - \overline{T_{LT}}\right), \tag{8}$$

where $\overline{T_{LT}}$ represents the translation vector between the coordinate system of the machine and the coordinate system of the LT.

$$\overline{T_{LT}} = \begin{pmatrix} oX_{LT} \\ oY_{LT} \\ oZ_{LT} \end{pmatrix}, \tag{9}$$

where $\overline{R_{LT}}$ represents the Olinde Rodrigues matrix θ between the LT and MT coordinate systems around the unitary vector u = (u_x, u_y, u_z), where $u_x^2 + u_y^2 + u_z^2 = 1$.

$$\overline{R_{LT}} = \begin{pmatrix} \cos(\theta) + u_x^2(1-\cos(\theta)) & u_x u_y(1-\cos(\theta)) - u_z\sin(\theta) & u_x u_z(1-\cos(\theta)) + u_y\sin(\theta) \\ u_x u_y(1-\cos(\theta)) + u_z\sin(\theta) & \cos(\theta) + u_y^2(1-\cos(\theta)) & u_y u_z(1-\cos(\theta)) - u_x\sin(\theta) \\ u_x u_z(1-\cos(\theta)) - u_y\sin(\theta) & u_y u_z(1-\cos(\theta)) + u_x\sin(\theta) & \cos(\theta) + u_z^2(1-\cos(\theta)) \end{pmatrix}, \tag{10}$$

where $\overline{X_{LT}}$ represents the coordinates of the machine point measured by using the LT.

$$\overline{X_{LT}} = \begin{pmatrix} X_{LT} \\ Y_{LT} \\ Z_{LT} \end{pmatrix}, \tag{11}$$

https://doi.org/10.1016/j.measurement.2018.10.012

where $\bar{T}$ is the offset of the tool.

$$\bar{T} = \begin{pmatrix} x_t \\ y_t \\ z_t \end{pmatrix}, \tag{12}$$

where $\overline{R_k}$ represents the rotational error matrix for axis k of the MT with *k = x, k = y* and *k = z.*

$$\overline{R_k} = \begin{pmatrix} 1 & -\varepsilon_{z,k} & \varepsilon_{y,k} \\ \varepsilon_{z,k} & 1 & -\varepsilon_{x,k} \\ -\varepsilon_{y,k} & \varepsilon_{x,k} & 1 \end{pmatrix}, \tag{13}$$

where $\bar{X}$ represents the linear error vector for the X-axis of the milling machine.

$$\bar{X} = \begin{pmatrix} -x + \delta_{x,x} \\ \delta_{y,x} \\ \delta_{z,k} \end{pmatrix}, \tag{14}$$

where $\bar{Y}$ represents the linear error vector for the Y-axis of the milling machine.

$$\bar{Y} = \begin{pmatrix} \delta_{x,y} - y \cdot S_{xy} \\ y + \delta_{y,y} \\ \delta_{z,y} \end{pmatrix}, \tag{15}$$

where $\bar{Z}$ represents the linear error vector for the Z-axis of the milling machine.

$$\bar{Z} = \begin{pmatrix} \delta_{x,z} - z \cdot S_{xz} \\ \delta_{y,z} - z \cdot S_{yz} \\ z + \delta_{z,z} \end{pmatrix}, \tag{16}$$

where $\varepsilon_{x,k}, \varepsilon_{y,k}$ and $\varepsilon_{z,k}$ are the three rotational errors of axis *k* (*k = x, k = y, k = z*); $\delta_{k,k}$ is the position error of axis *k* (*k = x, k = y, k = z*); $\delta_{k,j}$ with $k \neq j$ is the straightness error in the *k*-direction; and S_{xy}, S_{xz} and S_{yz} are squareness errors.

With the nominal coordinates of the calibrated plate, the measured coordinates are obtained by measuring 28 holes by using an LT (Leica LTD 600) and using the equations of the kinematic model. Hence, conducting a volumetric verification to determine the geometric errors of the system MT + LT is possible. These errors, which are mathematically modelled as second-order approximation functions, are used as generation functions on the simulation software used to determine the MT uncertainty by using the Monte Carlo method (owing to the size of the analysed MT working volume, using polynomials of higher order is unnecessary).

LT measurement noise is modelled as a normal distribution with 0 µrad as the mean value and 24 µrad as the 2-sigma value for angular encoders and 4 µm ± 0.8 µm/m for radial error. These values are selected in accordance with the LT manufacturer's documentation and several researcher's contributions [29].

The MT workspace to be verified is defined as a small area of the total MT workspace with dimensions of 0 mm ≤ X ≤ 400 mm, 0 mm ≤ Y ≤ 400 mm and Z = 0 mm (measurement area) based on the size of the plate. Considering these data and the approximation functions obtained previously, 1000 tests are performed.

Figure 7 shows the histograms of initial errors of the X-, Y-, Z-axes, as well as distance (i.e. total) error for the MT without any error compensation. The analysis of these results provides an average initial volumetric error of 77.39 µm with a standard deviation of 40.91 µm.

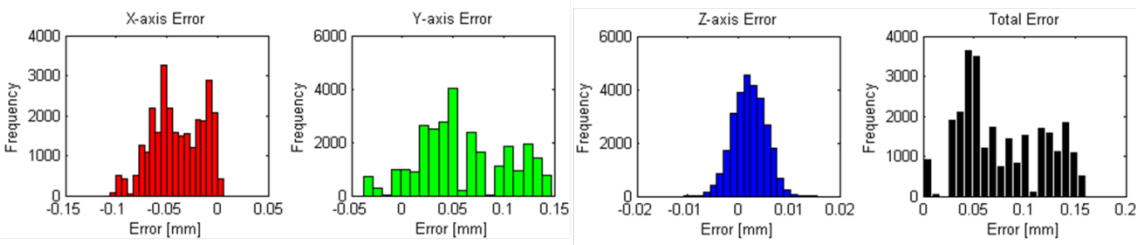

https://doi.org/10.1016/j.measurement.2018.10.012

Figure 7. *Initial error distribution*

These simulations show that the influence of the LT noise in the measured points affects the MT volumetric error and approximation functions obtained. Therefore, the final error of each point varies in each simulated test. By using the Monte Carlo method, the uncertainty of each point after the verification process can be obtained. The number of tests performed (n = 1000) is sufficient to observe the uncertainty trend.

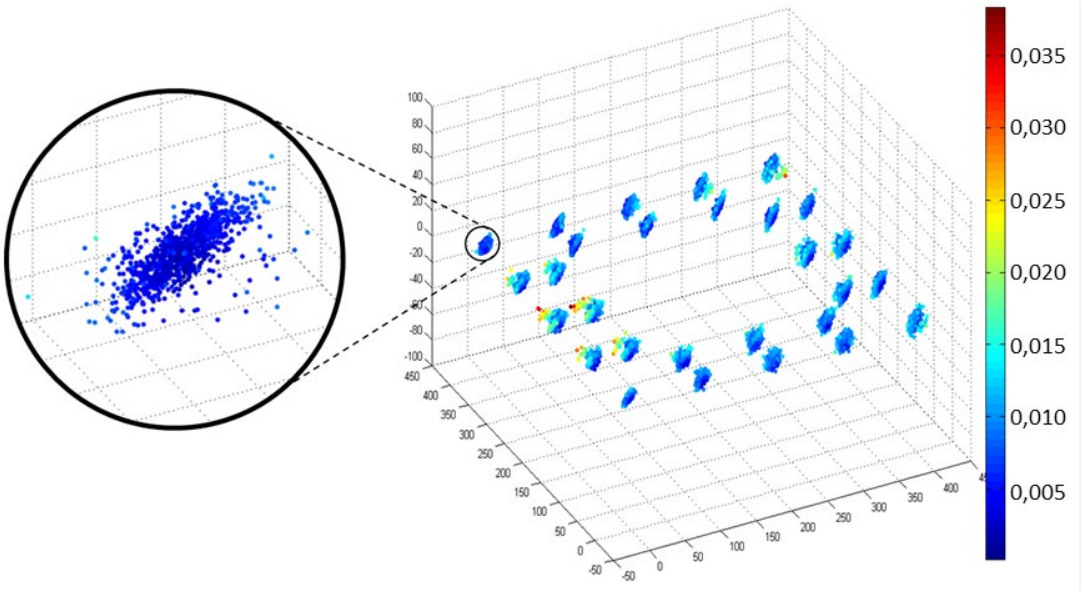

Figure 8. *Mesh of the simulated points*

Figure 8 shows the mesh of the simulated points obtained after applying nonlinear optimisation for each hole and trial generated. The points tend to form an ellipsoid characteristic of uncertainty, in which determining the true value of the measured point has high possibility.

As shown in Figure 9, the MT volumetric error has reduced substantially (compared with the initial error shown in Figure 7). Nonlinear optimisation can be used to reduce the MT errors. After applying the optimisation and compensating the errors, the average residual error has a normal biased distribution, positively skewed with a mean value of 12.34 µm and a standard deviation of 7.06 µm. The average residual error of each hole is regarded as a systematic error in that position of the MT workspace, whereas the standard deviation is part of the uncertainty of the measurement procedure (u_p).

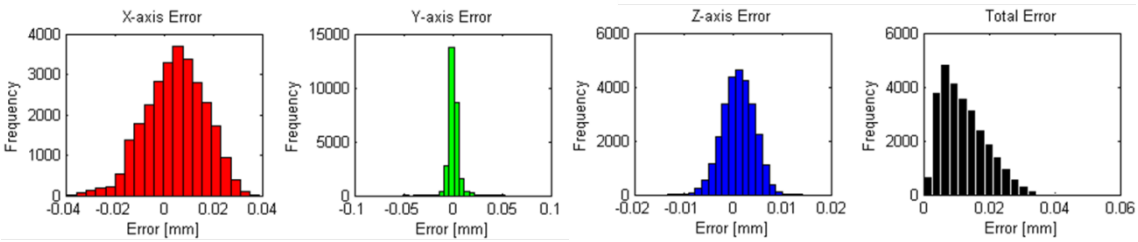

Figure 9. *Final error distribution*

By using the GUM [22], the measurement result should be expressed as follows:

$$Y = (y + b) \pm U, \tag{17}$$

where Y is the expression for the measurement, y is the measured value, b is the systematic error and U is the expanded uncertainty. Figure 9 shows the systematic error (b) in every position of the MT workspace.

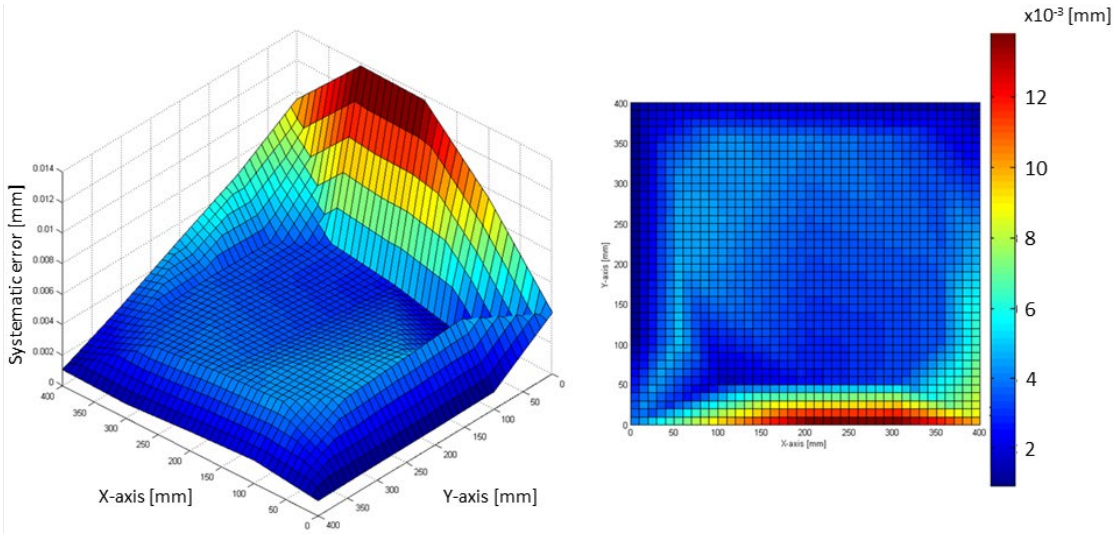

Figure 10. *Systematic error in the workspace*

Figure 10 shows the systematic error obtained in the simulation. The systematic error has values of approximately 2 µm, except along the X-axis, where the systematic error reaches a value of 14 µm. This result is caused by the squareness error and because the optimisation algorithm obtains the best global correction, but those points are absorbing the error.

Assuming that the accuracy of the sensor is ± 0.2 °C with a rectangular distribution, u_w can be calculated as follows:

$$u_w = \frac{\alpha \cdot \Delta T \cdot L}{\sqrt{3}} = \frac{24 \cdot 10^{-6} \cdot 0.2 \cdot 400}{\sqrt{3}} = 0.00111\ mm = 1.11\ \mu m. \quad (18)$$

The value of u_p for each position of the workspace is two times the standard deviation of the simulated mesh of points at that position (Figure 8). This is the most important source of uncertainty in this experiment. The expanded uncertainty can now be calculated for each workspace position. The results are shown in Figure 11.

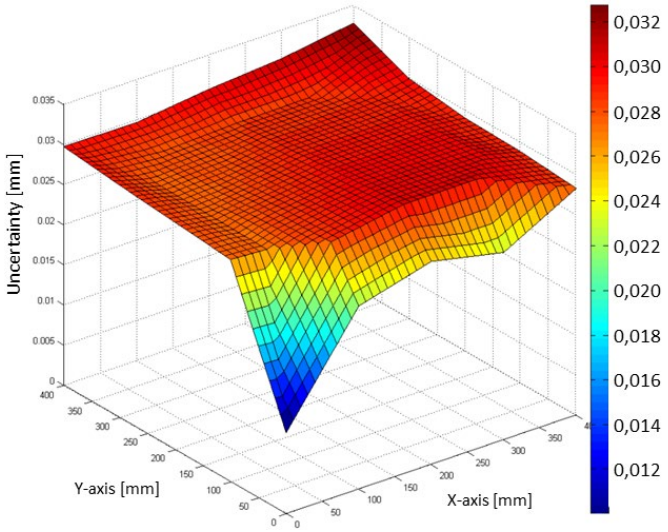

https://doi.org/10.1016/j.measurement.2018.10.012

Figure 11. *Expanded uncertainty of the workspace*

These results show the expanded uncertainty of each position of the workspace. The peak at position X = 0 mm and Y = 0 mm is owing to its particular condition as the origin of the coordinates. That is, this position is the point of reference for all the geometric errors and its uncertainty is lower. Meanwhile, the uncertainty is higher and homogeneous in the rest of the workspace. Further, the MT user can use the value of MPE of the MT to have information on the error in the distance measurements and not only in the position. Setting an MPE on the measurement system is one way of ensuring that when measurements are actually performed, the requirements on maximum permissible measurement uncertainty (MPU) are likely to be satisfied. Whether the MPU will be satisfied or is not depended not only on the instrument specifications but also on the actual metrological performance whilst measuring [30].

To estimate the MPE value for the measurement at various distances, the errors previously simulated were used. Different pairs of points were chosen, and their nominal distances were compared with the measured distances to determine the error per distance of the measurement. Three cases were investigated, namely, using all the data (coverage factor of 100%), using the values within the three standard deviations (coverage factor of 99%) and using the values within two standard deviations (coverage factor of 95%). Figure 12 shows the results of the comparison of the 1000 points corresponding to 55 pairs of centre distances of the holes; thus, information is available on the errors of 55000 distances.

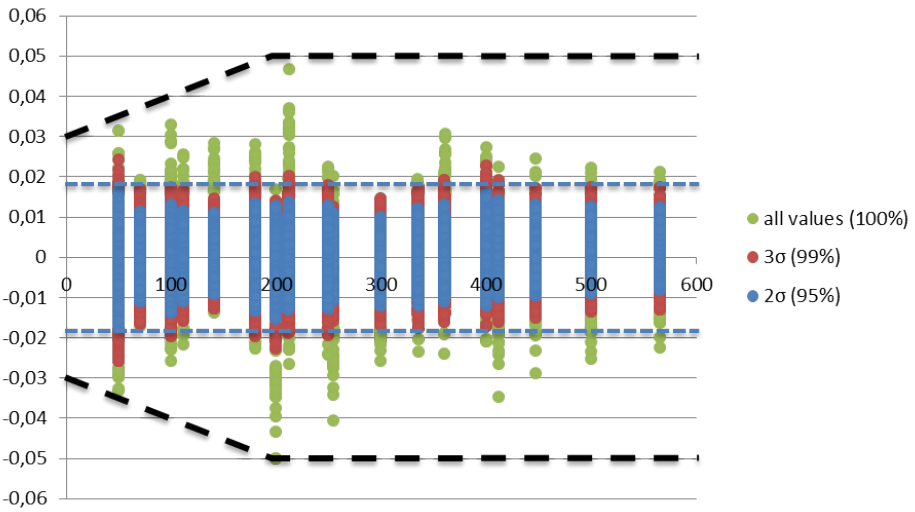

Figure 12. *Maximum permissible error*

The MPE of the MT is given by

$$\begin{cases} for\ 0 < L < 200\ mm\ ;\ MPE = (30 + \frac{L}{10})\ \mu m \\ for\ L > 200\ mm\ \ \ \ ;\ MPE = 50\ \mu m \end{cases}.$$

Alternatively, the value with a coverage factor of 95% can be used.

$$U_{95} = 17.5\ \mu m$$

5. Conclusions

The initial tests performed in this study show that the LT measurement noise has a significant influence on volumetric verification and provide calibration uncertainty related only to random errors introduced in the measured points. This source of uncertainty is normally neglected by a user, who assumes that

the errors provided by volumetric verification are perfectly accurate values. This source of uncertainty must be considered because of the increase in the uncertainty of the MT during the manufacturing and measuring processes.

Thus, the measurement data can be presented as the measured value, as well as a correction known as a residual volumetric error, and the uncertainty value. In a particular case of the MT considered in this study, within the workspace of 460 mm x 460 mm, the systematic error has values of approximately 2 µm. However, the uncertainty has an average value of approximately 30 µm in the entire workspace, except at the position where the origin of the coordinates has been set, where the expanded uncertainty has a minimum value of 12 µm. Apart from the information obtained for every point, the MT user may want to know the value of the MPE expected whilst measuring the distances. To estimate this value, several combinations of pairs of points are used. By comparing the measured distance with the nominal distance, the MPE value is estimated for three cases, that is, the absolute MPE and the MPE values with coverage factors of 99% and 95%. For a coverage factor of 95%, the MPE obtained is 17.5 µm. The uncertainties and MPEs estimated on this study are the result of noise in the measurement system (LT), and these must be added to the other sources of uncertainty to have a global view of the traceability of the MT.

When the MT is used as a measurement system, determining the measurement uncertainty is necessary. It is a quantitative indication of the quality of the measurement results, without which they cannot be compared between themselves, with specified reference values, or with the standard. In this paper, some of the sources with most influence over uncertainty have been studied, but in future work it would be interesting to study the influence of other factors such as temperature or the position of the laser tracker to have an overall vision of the measurement uncertainty.

Conflicts of interest

The authors declare no conflict of interest.

Acknowledgements

This work was supported by the Government of Spain with the project DPI2013-46979-C2-1-P: METRAP and the funds of the scholarship BES-2014-070480.

References

[1] A.P. Longstaff, S. Fletcher, S. Parkinson and A. Myers, The role of measurement and modelling of machine tools in improving product quality, Int. J. Metrol. Qual. Eng., 2013, 4, pp. 177-184.

[2] ASME B5.54-2005 Methods for Performance Evaluation of Computer Numerically Controlled Machining Centers.

[3] H. Schwenke, W. Knapp, H. Haitjema, A. Weckenmann, R. Schmitt, F. Delbressine, Geometric error measurement and compensation of machines – An update. CIRP Annals – Manufacturing Technology, 2008, 57(2), pp. 660-675.

[4] R. Ramesh, M.A. Mannan and A.N. Poo, Error compensation in machine tools – a review Part I: geometric, cutting-force induced and fixture-dependent errors, International Journal of Machine Tools & Manufacture, 2000, 40, pp. 1235-1256.

[5] ISO 841:2001 Industrial Automation Systems and Integration – Numerical Control of Machines – Coordinate System and Motion Nomenclature.

[6] VDI/VDE 2617-3 (1989) Accuracy of Coordinate Measuring Machines: Characteristic Parameters and Their Checking Components of Measurement Deviation of the Machine.

[7] UNE-ISO 230-1:2014 Geometric accuracy of machines operating under no-load or quasi-static conditions.

[8] S. Aguado, D. Samper, J. Santolaria, J.J. Aguilar. Towards an effective strategy in volumetric error compensation of machine tools. Measurement Science and Technology, 2012, 23, 12pp. doi:10.1088/0957-0233/23/6/065003

[9] S. Aguado, J. Santolaria, D. Samper, J. Aguilar, J. Velazquez, Improving a real milling machine accuracy through an indirect measurement of its geometric errors, Int. Journal of Manufacturing Systems, 2016, 40, pp. 26-36.

[10] E. Trapet, F. Wäldele, A reference object based method to determine the parametric error components of coordinate measuring machines and machine tools. Measurements, 1991, 9(1), pp. 17-22.

[11] H. Schwenke, C. Warmann, High Speed High Accuracy Multilateration System Based on Tracking Interferometers, 10th IMEKO TC14 Symposium on Laser Metrology for Precision Measurement and Inspection in Industry, Braunschweig (Germany), 2011, September 12-14.

[12] M. Uekita, Y. Takaya, On-machine dimensional measurement of large parts by compensating for volumetric errors of machine tools, Precision Engineering, 2016, 43, pp. 200-210.

[13] F. Ezedine, J.M. Linares, J.M. Sprauel, J. Chaves-Jacob, Smart sequential multilateration measurement strategy for volumetric error compensation of an extra-small machine tool, Precision Engineering, 2016, 43, pp. 178-186.

[14] S. Aguado, D. Samper, J. Santolaria, J.J. Aguilar, Machine Tool Rotary Axis Compensation Through Volumetric Verification Using Laser Tracker, Proceedings of 5th Manufacturing Engineering Society International Conference (MESIC 2013). Zaragoza (Spain), 2013. doi: 10.1016/j.proeng.2013.08.189.

[15] Z. Wang, P.G. Maropolous, Real-time error compensation of a three-axis machine tool using a laser tracker, Int J Adv Manuf Technol, 2013, 69, pp. 919–933.

[16] A. Wan, L. Song, J. Xu, S.Liu, K. Chen, Calibration and compensation of machine tool volumetric error using a laser tracker, International Journal of Machine Tools and Manufacture, 2018, 124, pp. 126–133.

[17] H.J. Pahk, Y.S. Kim, J.H. Moon, New Technique for Volumetric Error Assessment of CNC Machine Tools Incorporating Ball Bar Measurement and 3D Volumetric Error Model, International Journal of Machine Tools and Manufacture, 1997, 37, pp. 1583-1596.

[18] A.B. Forbes, Measurement uncertainty and optimized conformance assessment, Measurement, 2006, 39(9), pp. 808–814.

[19] J.E. Muelaner, M. Chappell, P.S. Keogh, A unified approach to uncertainty for quality improvement, 12th International Conference and Exhibition on Laser Metrology, Machine Tool, CMM and Robotic Performance, LAMDAMAP 2017, EUSPEN, pp. 164-174.

[20] ISO/TR 230-9:2005 Estimation of measurement uncertainty for machine tool tests according to series ISO 230, basic equations.

[21] ISO 14253-2-2011 Inspection by measurement of workpieces and measuring equipment -- Part 2: Guidance for the estimation of uncertainty in GPS measurement, in calibration of measuring equipment and in product verification.

[22] Evaluation of measurement data: Guide to the expression of Uncertainty in Measurement (GUM). JCGM 100:2008.

[23] T. Liebrich, B. Bringmann, W. Knapp, Calibration of a 3-D ball plate, Precision Engineering, 2009, 33(1), pp. 1-6. DOI: 10.1016/j.precisioneng.2008.02.003

[24] M. Jankowski, A. Woźniak, Master artifacts for testing the performance of probes for CNC machine tools, Advanced Mechatronics Solutions, Part of the Advances in Intelligent Systems and Computing book series (AISC, volume 393), pp. 323-328. DOI 10.1007/978-3-319-23923-1_49

[25] B. Štrbac, V. Radlovački, B. Ačko, V. Spasić – Jokić, Lj. Župunski, M. Hadžistević, The use of Monte Carlo simulation in evaluating the uncertainty of flatness measurement on a CMM, Journal of Production Engineering, 2016, 19(2), pp. 69-72.

[26] J. Santolaria, M. Ginés. Uncertainty estimation in robot kinematic calibration. Robotics and Computer-Integrated Manufacturing, 2013, 29, pp. 370-384.

[27] ISO/TR 15530-3:2011 Coordinate measuring machines (CMM): Technique for determining the uncertainty of measurement – Part 3: Use of calibrated workpieces or measurement standards.

https://doi.org/10.1016/j.measurement.2018.10.012

[28] P. Pérez, J.A. Albajez, J. Santolaria, Analysis of the initial thermal stabilization and air turbulences effects on Laser Tracker measurements, Int. Journal of Manufacturing Systems, 2016, 41, pp. 277-286.

[29] H. Zhuang, S. H. Motaghedi, Z. S. Roth, Y.Bai. Calibration of multi-beam laser tracking systems. Robotics and Computer-Integrated Manufacturing, 2003, 19, pp. 301-314.

[30] A.M. Joglekar, Statistical methods for six sigma in R&D and manufacturing, 2003. Wiley, Hoboken ISBN: 0-471-20342-4.